**CERN - European Organization for Nuclear Research**

**LCD-Note-2011-029**

# Occupancy in the CLIC_ILD Time Projection Chamber

Martin Killenberg*

* *CERN, Switzerland*

July 4, 2012

## Abstract

We report on the occupancy in the CLIC_ILD TPC caused by the beam induced background from $\gamma\gamma \rightarrow$ hadrons, $e^+e^-$ pairs and beam halo muons. In addition the particle composition of the backgrounds and the origin of backscattering particles have been studied.

# 1. Introduction

For the CLIC_ILC detector a Time Projection Chamber (TPC) is forseen as the main tracking device [1]. Due to its long readout time of $\mathcal{O}(30\ \mu s)$ the TPC integrates over a full CLIC bunch train, which only lasts 156 ns. To estimate the occupancy, the beam induced background has been simulated in the Geant4-based full detector simulation Mokka [2]. Mokka does not only calculate the charge deposition of primary particles from the vertex, but also of particles scattering back from other detector components.

The occupancy has been calculated from the simulated ADC response. The digitisation has been performed with the MarlinTPC package [3], which takes into account diffusion in the gas, charge broadening in the gas amplification structure and the shaping of the electronics to simulate realistic TPC raw data. For this study a triple GEM stack and a charge sensitive ADC with 40 MHz readout frequency have been used. A detailed description of the software and the simulation parameters can be found in a dedicated note [4].

The occupancy is measured as the fraction of voxels (3D space buckets) which contain a signal. The size of a voxel corresponds to the size of a readout pad in the $xy$ plane, and to one time sample of the ADC in the $z$ direction, multiplied with the electron drift velocity in the gas ($25\ \text{ns} \cdot 79\ \text{mm}/\mu\text{s} \approx 2\ \text{mm}$.) The exact values of all parameters can also be found in the software note [4].

All results in this study are based on a full CLIC bunch train with 312 bunch crossings (BX) and the following backgrounds:

- 300.000 $e^+e^-$ pairs per BX
- 3.2 $\gamma\gamma \rightarrow$ hadrons events per BX
- 1 beam halo muon per BX

These values correspond to the results of the respective beam background studies without safety factors [5]. One beam halo muon per bunch crossing is a conservative estimate [6].

# 2. Occupancy in the TPC

The occupancy is shown for a pad size of $1 \times 6\ \text{mm}^2$, which is the pad size in the CLIC_ILD_CDR detector model. The influence of the pad size on the occupancy is discussed in section 2.1.

The average voxel occupancy, calculated for all pads and $z$ bins of one pad row, as a function of the pad row is shown in figure 1a. The contributions from the three different background types are shown separately, as well as the overall occupancy. The dominating contribution is the $\gamma\gamma \rightarrow$ hadrons background with up to 25 % occupancy in the innermost pad rows, followed by the $e^+e^-$ pair background with 10 % in the inner pad rows. The contribution from beam halo muons is negligible compared to the other two components.

The overall occupancy drops from 30 % in the inner pad rows to 1 % at the outer radius of the TPC. From pad row 50 on (corresponding to a radius of 70 cm) the occupancy is below 10 %.

The values in figure 1a average over all $z$ bins. Unfortunately the distribution along $z$ is not uniform, as figure 1b shows. Here the occupancy for all background components is plotted as

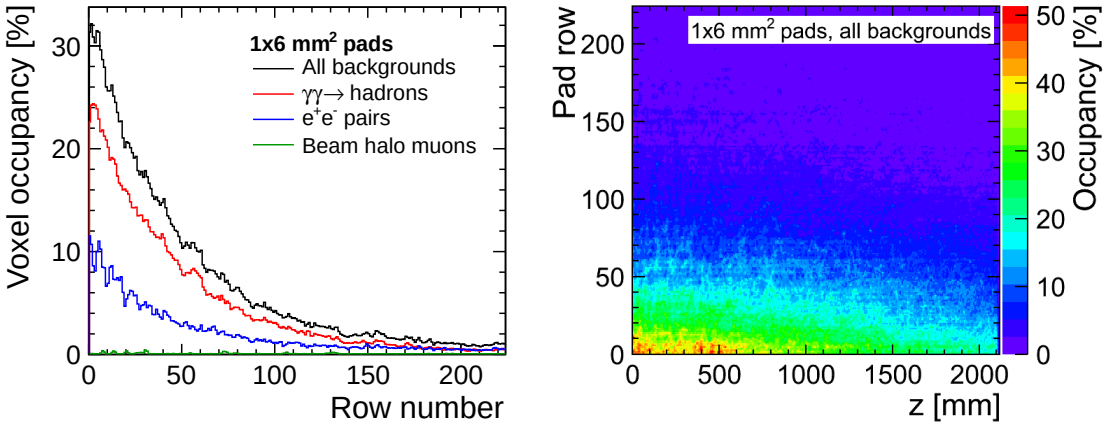


(a) The voxel occupancy calculated per pad row.

(b) The voxel occupancy calculated per pad row and $z$ bin.

Figure 1: The TPC's voxel occupancy for one bunch train of the different background components as a function of the pad row, and as a function of the pad row and $z$ for all background components. The values are calculated for a pad size of $1 \times 6$ mm$^2$.

a function of the $z$ coordinate and the pad row. The averaging is only done in $\phi$ direction. The local occupancy in the inner pad rows near the cathode goes up to 50 %, as the local track density is higher near the interaction point. But the occupancy near the end plate is only around 20 %, which still allows the detection of tracks in the forward direction even if the central region of the TPC might not be usable any more.

Table 1 summarises the average occupancies in the inner 10 pad rows, as well as the overall average occupancy which is 4.7 %, with 3.3 % originating from the $\gamma\gamma \rightarrow$ hadrons and 1.5 % from the $e^+e^-$ pairs background. The contribution from the beam halo muons with only 0.05 % is smaller than the uncertainties on the other components and can be neglected.

The pad occupancy (table 2) in the inner pad rows is 100 %, so every single pad has a signal at a certain time during the TPC readout cycle. Even the average overall pad occupancy is almost 80 %.

For the pattern recognition not only the average occupancy per pad row is interesting, but also the distribution of occupancies for single pads. It has been shown that low-energetic particles for instance, which curl within one pad row, can be rejected efficiently at an early stage of the reconstruction [7].

Figure 2 shows the occupancy for each readout channel of one TPC end plate, overall and separately for the three background components. The $\gamma\gamma \rightarrow$ hadrons background mainly causes occupancies of up to 20 % on a pad, but drops towards signals which occupy one pad for a larger fraction of the total readout time. Signals from the $e^+e^-$ pair background on the other hand leads to a higher fraction of pads with a large occupancy, and creates a small peak at 100 %, where the pad has a signal in all of its voxels.The reason is that most of the particles from this background

| Background | Pad rows | Occupancy [%] | ( nOccupied / | nVoxels) |
|---|---|---|---|---|
| all | all | 4.66 | (75,127,567 / | 1,612,737,732) |
| | inner 10 | 29.9 | ( 8,574,744 / | 28,673,652) |
| $\gamma\gamma \to$ hadrons | all | 3.30 | (53,140,404 / | 1,612,737,732) |
| | inner 10 | 22.7 | ( 6,520,157 / | 28,673,652) |
| $e^+e^-$ pairs | all | 1.45 | (23,317,395 / | 1,612,737,732) |
| | inner 10 | 9.34 | ( 2,678,586 / | 28,673,652) |
| beam halo muons | all | 0.0524 | ( 845,013 / | 1,612,737,732) |
| | inner 10 | 0.10 | ( 29,469 / | 28,673,652) |

Table 1: The average voxel occupancies per pad row in the TPC for the different types of beam induced background at a pad size of $1 \times 6$ mm$^2$.

| Background | Pad rows | Occupancy [%] | (nOccupied / | nPads) |
|---|---|---|---|---|
| all | all | 77.7 | ( 1,166,452 / | 1,501,618) |
| | inner 10 | 100 | ( 26,698 / | 26,698) |
| $\gamma\gamma \to$ hadrons | all | 72.2 | ( 1,084,454 / | 1,501,618) |
| | inner 10 | 100 | ( 26,698 / | 26,698) |
| $e^+e^-$ pairs | all | 31.1 | ( 466,918 / | 1,501,618) |
| | inner 10 | 88.3 | ( 23,586 / | 26,698) |
| beam halo muons | all | 0.59 | ( 8,824 / | 1,501,618) |
| | inner 10 | 0.96 | ( 257 / | 26,698) |

Table 2: The average pad occupancies in the TPC for the different types of beam induced background at a pad size of $1 \times 6$ mm$^2$.

type are backscattered photons (see section 3) which cause the afore mentioned low-energetic curlers when they convert inside the TPC. The beam halo muons do not propagate exactly along one pad because they are basically parallel to the incoming beam, which has a 10 mrad angle with respect to the detector axis.

To get an impression where the high occupancy region of the inner pad rows is located inside the spectrum, figure 3 shows the spectra for $\gamma\gamma \to$ hadrons, $e^+e^-$ pair background and all background components separated into pad row groups with increasing radius. The $\gamma\gamma \to$ hadrons background shows a maximum at 15 % occupancy per pad for the inner pad rows. Towards larger radii the occupancy on a single pad is shifting towards smaller values. This can be understood because particles coming from the interaction region in a shallow angle turn on more voxels per pad than particles with a large polar angle, which also reach the outer pad rows.

The $e^+e^-$ pair background does not show large differences between inner and outer pad rows.

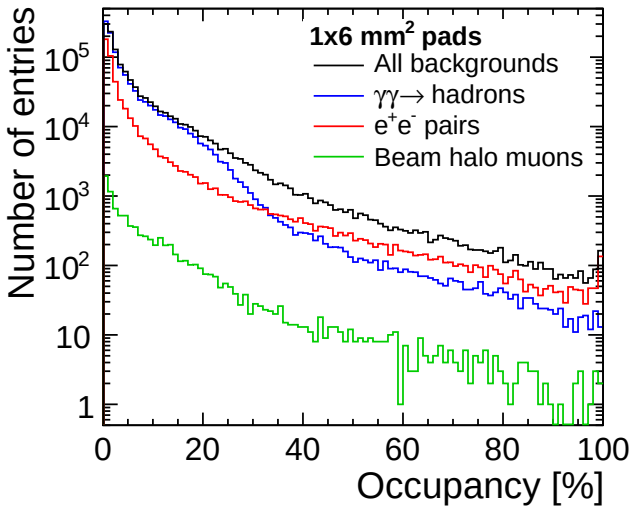


Figure 2: The pad occupancy spectra for the three background components at a pad size of $1 \times 6$ mm$^2$. The histogram only contains channels which see a signal, corresponding to 78 %, 72 %, 31 % and 0.6 % of all channels, respectively (see table 2). Empty channels are not considered.

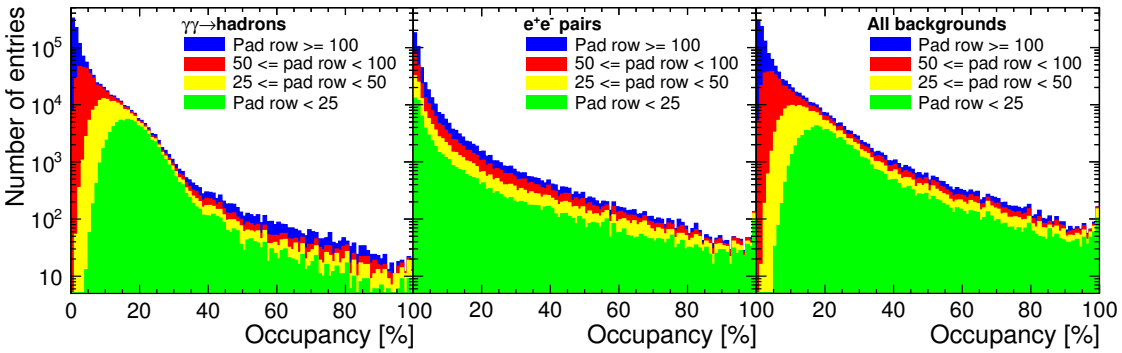


Figure 3: The pad occupancy spectra for $\gamma\gamma \rightarrow$ hadrons, $e^+e^-$ pair background and all background components for a pad size of $1 \times 6$ mm$^2$, separated into groups of pad rows.

Again this can be understood because this background component mainly consists of photons causing low-energetic curlers (see section 3), which give the same occupancy spectrum per pad, independent from the radius.

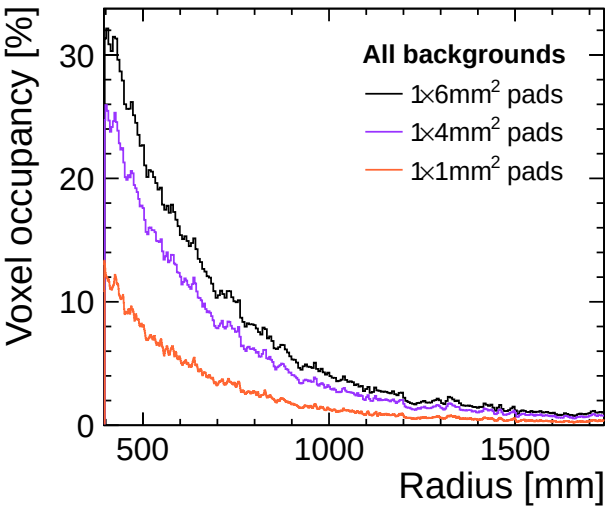


Figure 4: The average TPC occupancy per pad row for different pad sizes for one bunch train of beam induced background of all background components.

## 2.1. Occupancy for Different Pad Sizes

Figure 4 shows the average occupancy per pad row for the sum of all three background components for three different pad sizes: $1 \times 6$ mm$^2$, $1 \times 4$ mm$^2$ and $1 \times 1$ mm$^2$. For completeness the plots and occupancy values for the individual background components are given in appendix A. As expected, the occupancy decreases for smaller pad sizes. The occupancy in the inner pad rows goes down from 30 % for $1 \times 6$ mm$^2$ pads to 25 % for $1 \times 4$ mm$^2$ pads and to 12 % for $1 \times 1$ mm$^2$ pads. It is interesting to see that the occupancy does not scale linearly with the pad size. While there is a factor 6 between the largest and the smallest pad size, the occupancy only goes down by a factor 2.5. The maximum occupancy of 12 %, however, is a much more relaxed condition for the pattern recognition.

With current electronics a pad size of $1 \times 1$ mm$^2$ cannot be implemented. Further R&D would be required to reach the high electronics integration and to ensure a sufficient signal to noise ratio, as pulse heights are lower for smaller pads. Another option is to go for a pixelised TPC readout, where the charge is directly collected onto the bump bond pads of a readout ASIC. Current R&D with the Timepix chip, which has a pad size of $55 \times 55$ µm$^2$, shows very promising results.

## 2.2. Space Charge in the TPC

The high occupancy leaves a cloud of ions in the TPC which drift slowly towards the cathode. Figure 5 shows the mean space charge (average charge per volume) for one bunch train of beam

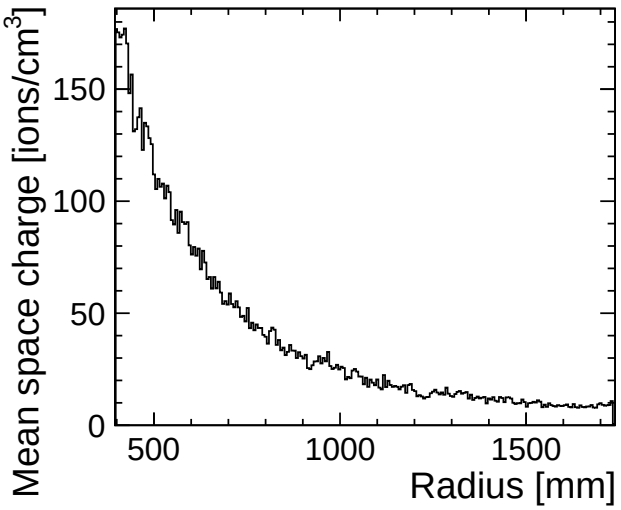


Figure 5: The mean space charge of primary ions from one bunch train of beam induced background in the TPC as a function of the radius, calculated for the volume read out by one pad row for $1 \times 6$ mm$^2$ pads.

induced background at CLIC, calculated for the volume which is read out by one pad row.[1)] For the inner radii the charge is more than 170 ions per cm$^3$, which is almost a factor 10 higher than at the ILC for the same number of bunch crossings [8]. With a drift time of up to one second there are primary ions from up to 50 bunch trains in the TPC at CLIC. The ILC, with ten times more bunch crossings per train but a repetition rate of only 5 Hz, has approximately the same number of bunch crossings per second as the CLIC accelerator.

The impact of the space charge on the field quality is currently being studied.

## 3. Composition of the Background

The generated signal and the amount of charge deposited in the TPC depend on the particle type. High-energetic charged particles leave a trace of ionised gas atoms along their path, while photons will produce low-energetic electrons which leave narrow curlers propagating along the magnetic field lines. Neutrons mainly create low-energetic protons when they collide with hydrogen atoms in the gas, leaving small track stubs in the TPC.

Table 3 lists the different types of particles which leave a signal in the TPC, separately for the three background types. It gives the number of particles and the energy which is deposited by this particle type in one bunch train. The results are also visualised in figures 6 and 7 (number of particles and deposited energy, respectively).

The largest contribution are photons from the $e^+e^-$ pair background. More than 120,000

[1] For $1 \times 6$ mm$^2$ pads

| Particle type | $\gamma\gamma \to$ hadrons Count | $\gamma\gamma \to$ hadrons $E_{\text{dep}}$ [GeV] | $e^+e^-$ pairs Count | $e^+e^-$ pairs $E_{\text{dep}}$ [GeV] | Beam halo muons Count | Beam halo muons $E_{\text{dep}}$ [GeV] |
|---|---|---|---|---|---|---|
| $e^{\pm}$ | 984 | 1.11 | 1502 | 0.790 | 57 | 0.0640 |
| $\mu^{\pm}$ | 223 | 0.172 | - | - | 75 | 0.107 |
| $\gamma$ | 6628 | 1.34 | 123222 | 14.6 | 838 | 0.133 |
| $K^0_{\text{long}}$ | 17 | 0.145 | - | - | - | - |
| $\pi^{\pm}$ | 4523 | 3.75 | - | - | - | - |
| $K^{\pm}$ | 489 | 0.444 | - | - | - | - |
| n | 5008 | 0.650 | 10176 | 0.516 | 3 | $6.57 \cdot 10^{-5}$ |
| p | 1260 | 3.28 | 8 | 0.0225 | - | - |
| pnnn[2] | 22 | 0.134 | - | - | - | - |
| sum | 19154 | 11.0 | 134908 | 15.9 | 973 | 0.304 |

Table 3: The number of different particles entering the TPC for one bunch train of beam induced background, and the total energy deposited in the TPC by this type of particle.

[2] The pnnn is an intermediate state with PDG ID 1000010048, consisting of one proton and three neutrons, which has not decayed yet when entering the TPC.

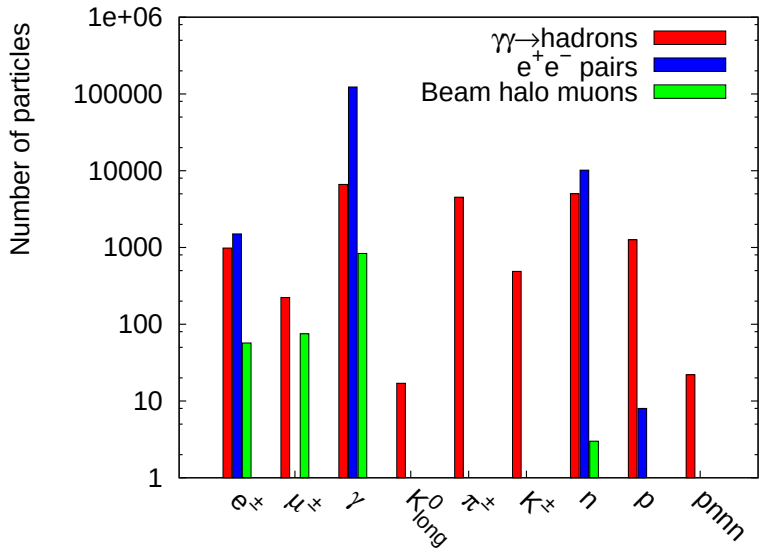


Figure 6: The number of different particles from the three background components for one bunch train.

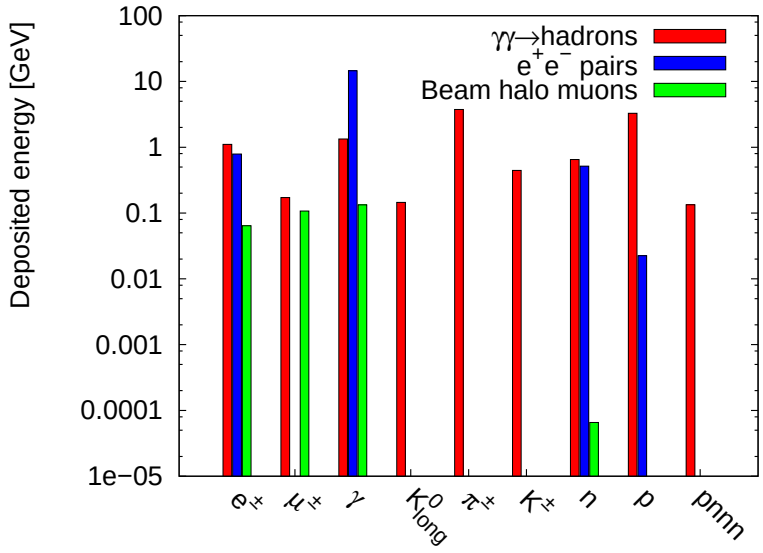


Figure 7: The energy deposited in the TPC by different types of particles from the three different backgrounds for one bunch train.

photons deposit an energy of almost 15 GeV per bunch train in the TPC. The direct deposition from electrons and positrons is comparatively small for this background type (see also table 4).

For the $\gamma\gamma \rightarrow$ hadrons background the largest energy depositions originate from ~4500 charged pions (3.8 GeV) and ~1300 protons (3.3 GeV).

It is interesting that the total energy deposition of 11 GeV from the $\gamma\gamma \rightarrow$ hadrons background is lower than the 16 GeV deposited by the $e^+e^-$ pair background, although the occupancy caused by the $\gamma\gamma \rightarrow$ hadrons is much higher. The reason is that the high-energetic charged particles from the $\gamma\gamma \rightarrow$ hadrons background are almost minimum ionising and leave less charge per track length than the low-energetic electrons produced by the photons from the $e^+e^-$ pairs.

The energy deposition from the 15,000 neutrons (5,000 from $\gamma\gamma \rightarrow$ hadrons and 10,000 from $e^+e^-$ pairs) is more than one order of magnitude below the total energy deposition in the TPC.

## 4. Origin of the Background Particles

The particles from $\gamma\gamma \rightarrow$ hadrons events and $e^+e^-$ pairs are coming from the interaction point. The beam halo muons used in this simulation are coming from the "scoring plane" of the beam halo simulation, which is the exit of the QF1 quadrupole [9][6]. This plane is approximately 10 m upstream of the interaction point. The particles which leave signals in the TPC, however, are not necessarily particles directly originating from the IP, or the beam halo muons themselves, but can be backscattered particles from other detector components. In the case of $e^+e^-$

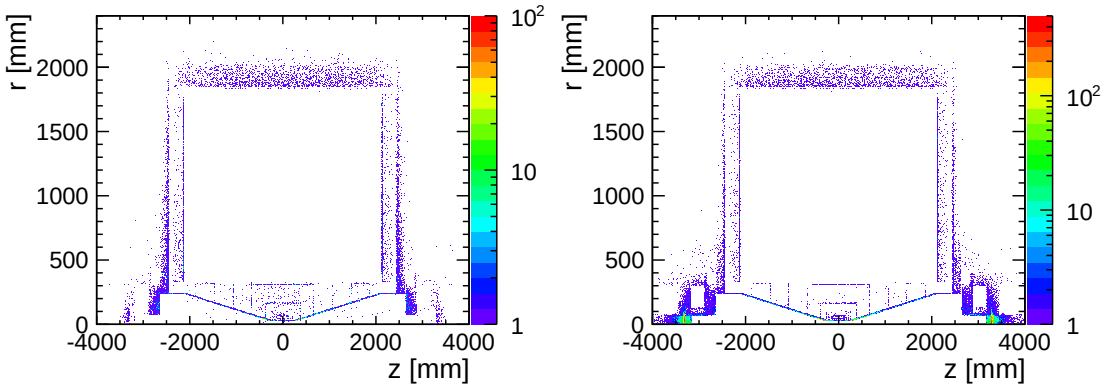


(a) $\gamma\gamma \to$ hadrons

(b) $e^+e^-$ pairs

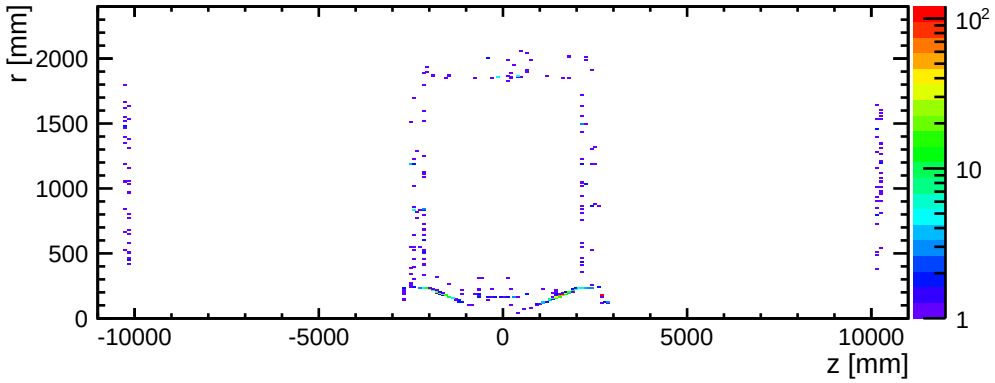


(c) Beam halo muons

Figure 8: Origins of the particles which leave an energy deposition in the TPC.

pair background this even is the majority. To visualise where the particles come from, for each `SimTrackerHit` in the TPC the `MCParticle` entering the TPC has been determined and stored in a list.[3)] The locations of the `MCParticle` vertices are shown in figure 8. For all three background components one observes that there are backscattered particles from basically all detector components. The inner edge of the ECal is visible, as well as the TPC end plate, the silicon tracking detectors and the beam pipe. Especially for the beam halo muons (figure 8c) the beam pipe is the major source of scattering particles.

For the $\gamma\gamma \to$ hadrons and $e^+e^-$ pairs figure 9 shows a zoomed view of the region up to the inner field cage of the TPC. For the $\gamma\gamma \to$ hadrons the hottest area is the inner edge of the conical part of the beam pipe. This is not surprising since it is a beam pipe pointing to the IP and all

[3]The algorithm follows the Monte Carlo truth list until it finds the first particle with an origin outside the TPC's fiducial volume. For $\delta$-electrons for instance the particle which created the delta electron is listed.

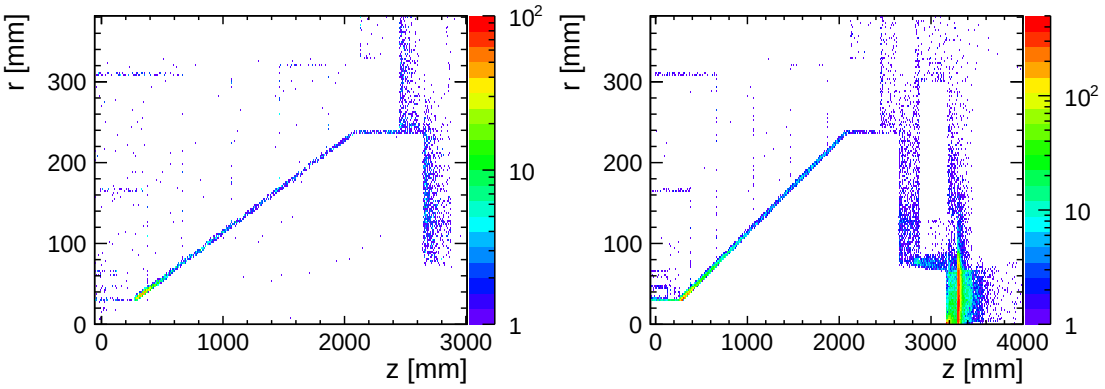


(a) $\gamma\gamma \rightarrow$ hadrons

(b) $e^+e^-$ pairs

Figure 9: Zoomed view of the origins of the particles which leave an energy deposition in the TPC.

particles in this particular angular region hit the inner edge of the beam pipe. Barely visible, since only one bin in the picture, is the interaction point itself, from which about one quarter of the particles of the $\gamma\gamma \rightarrow$ hadrons background are coming.

The $e^+e^-$ pairs are also coming from the interaction point, thus also here the inner edge of the beam pipe is a source of scattering particles. But the major contribution are the particles scattering back from the BeamCal. As table 3 shows they are basically all photons. The *xy* view of the particles scattering back from the *z* region which corresponds to the BeamCal (figure 10) clearly shows that the hot area is around the outgoing beam pipe. The fact that a large fraction of hits from the $\gamma\gamma \rightarrow$ hadrons background is directly coming from particles from the IP and the majority of hits from $e^+e^-$ pairs are backscattered particles also reflects in the time structure of the hits (figure 11). Most of the hits for $\gamma\gamma \rightarrow$ hadrons are created within 10 ns after the collision, while for $e^+e^-$ pairs the maximum is between 20 and 30 ns, which corresponds to the time of flight to the BeamCal and back into the TPC.

In section 3 we have seen that the energy deposition in the TPC does not scale linearly with the number of particles but also depends on the particle composition. Figure 12 shows the energy deposition in the TPC, histogrammed at the origin of the particles which are entering the TPC and separated by the different background components. Again, the beam pipe shows up as a hot area, as well as the BeamCal for the $e^+e^-$ pair background.

Table 4 lists the number of particles coming from the IP (or the scoring plane in the case of the beam halo muons) and the total number of particles for the respective background type. For the $\gamma\gamma \rightarrow$ hadrons about one quarter of the particles directly comes from the interaction point, producing about one third of the energy deposition from this background type. For the $e^+e^-$ pair background the contribution of direct particles is negligible. 75 beam halo muons enter the TPC directly, leaving around one third of the energy deposition from this background component. The almost nine hundred scattered particles leave only twice as much energy in the TPC.

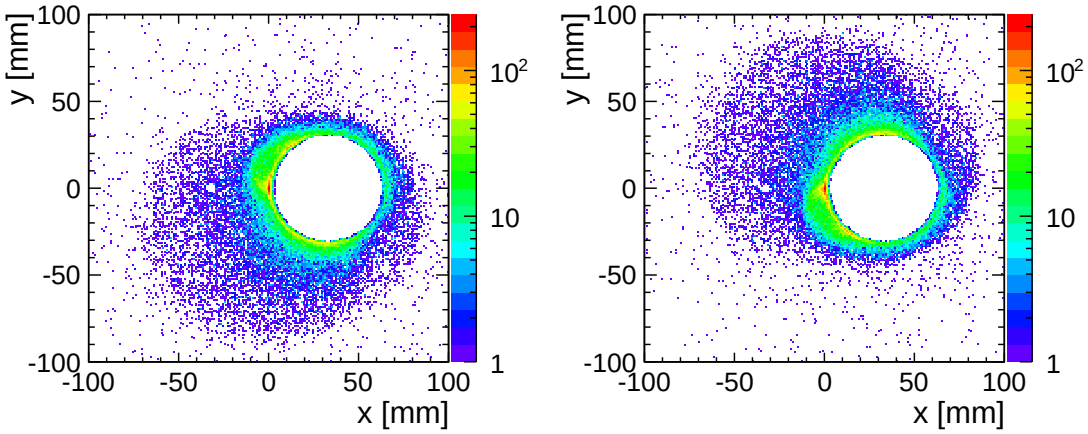


(a) Positive $z$ direction

(b) Negative $z$ direction

Figure 10: Origins of backscattering particles from the BeamCal which reach the TPC.

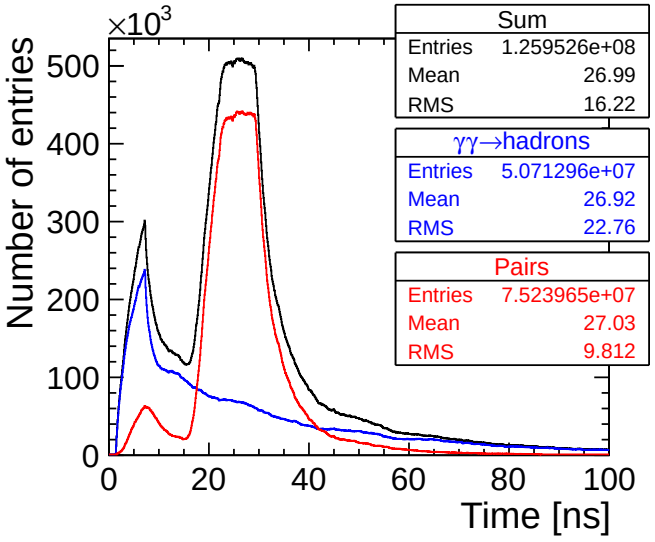


Figure 11: The time distribution of the hits in the TPC from $\gamma\gamma \to$ hadrons and $e^+e^-$ pair background.

## 5. Conclusions

At the default pad size of $1 \times 6$ mm$^2$ the average occupancy in the inner pad rows shows a high value of 30 % for a full bunch train of beam induced background at a 3 TeV CLIC machine. The main contribution is the $\gamma\gamma \to$ hadrons background, followed by $e^+e^-$ pair background.

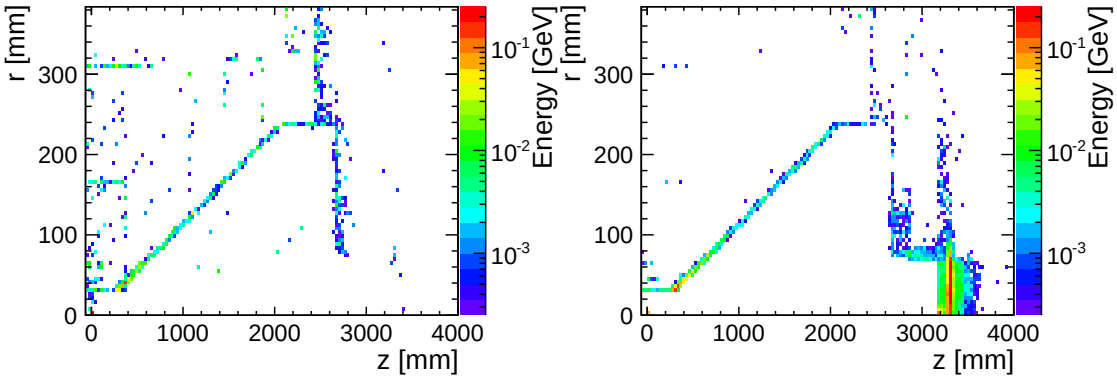


(a) $\gamma\gamma \to$ hadrons

(b) $e^+e^-$ pairs

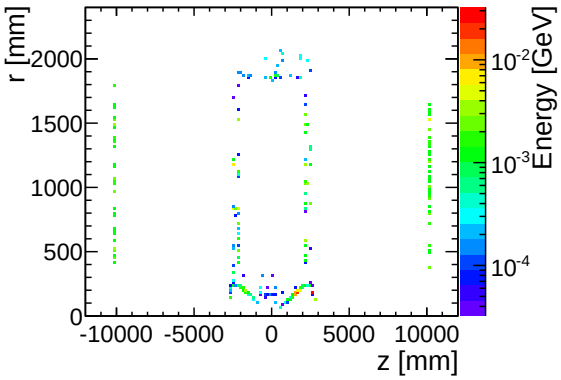


(c) Beam halo muons

Figure 12: Energy deposited in the TPC, histogrammed at the origin of the particles which are entering the TPC.

| | From source | | Total | |
|---|---|---|---|---|
| Background | Count | $E_{\text{dep}}$ [GeV] | Count | $E_{\text{dep}}$ [GeV] |
| $\gamma\gamma \to$ hadrons | 4770 | 4.06 | 19154 | 11.0 |
| $e^+e^-$ pairs | 176 | 0.0717 | 134908 | 15.9 |
| beam halo muons | 75 | 0.107 | 973 | 0.304 |

Table 4: The number of particles directly coming from the source of the background (IP or beam halo muons scoring plane), the total number of primary and secondary particles of the respective background and the corresponding energy depositions in the TPC for one bunch train.

The contribution from beam halo muons is negligible. Towards larger radii the voxel occupancy drops quickly. For $r > 70$ cm the mean occupancy per pad row is below 10 %, and the average value for the whole TPC is 4.7 %.

Using smaller pad sizes the occupancy can be reduced significantly. For $1 \times 1$ mm$^2$ pads the occupancy in the inner pad rows goes down to 12 %. Implementing such a small pad size, however, requires further R&D on the electronics. A pixelised TPC readout seems another viable solution.

The thick pointing beam pipe is a significant source of scattering. For the $e^+e^-$ pair background the main source of signal in the TPC are backscattering photons from the BeamCal. For the design of the beam pipe and the BeamCal the background in the TPC has not been taken into account. A careful redesign might help to reduce the TPC occupancy.

## References


[1] A. Münnich and A. Sailer. The CLIC_ILD_CDR Geometry for the CDR Monte Carlo Mass Production. LCD-Note-2011-002, 2011.

[2] Mokka, a detailed Geant4 simulation for the International Linear Collider detectors. Website: http://ilcsoft.desy.de/portal/software_packages/mokka/.

[3] MarlinTPC, Marlin based simulation, digitisation, reconstruction and analysis code for the TPC. Website: http://ilcsoft.desy.de/portal/software_packages/marlintpc/.

[4] M. Killenberg. Software and parameters for detailed TPC studies in the CLIC CDR. LCD-Note-2011-025, 2011.

[5] D. Dannheim and A. Sailer. Beam-induced backgrounds in the CLIC detectors. LCD-Note-2011-021, 2011.

[6] The CLIC accelerator design: Conceptual Design Report, in preparation.

[7] The LCTPC collaboration. The Linear Collider Time Projection Chamber of the International Large Detector. Report to the Desy PRC, 2010.

[8] A. Vogel. *Beam-Induced Backgrounds in Detectors at the ILC*. Ph.D. thesis, 2008. http://www-library.desy.de/cgi-bin/showprep.pl?desy-thesis-08-036.

[9] CLIC muon background simulation using BDSIM. Website: https://www.pp.rhul.ac.uk/twiki/bin/view/JAI/ClicMuon.

# A. Detailed Plots and Tables for the $1 \times 4$ mm$^2$ and $1 \times 1$ mm$^2$ Pads

## A.1. $1 \times 4$ mm$^2$ Pads

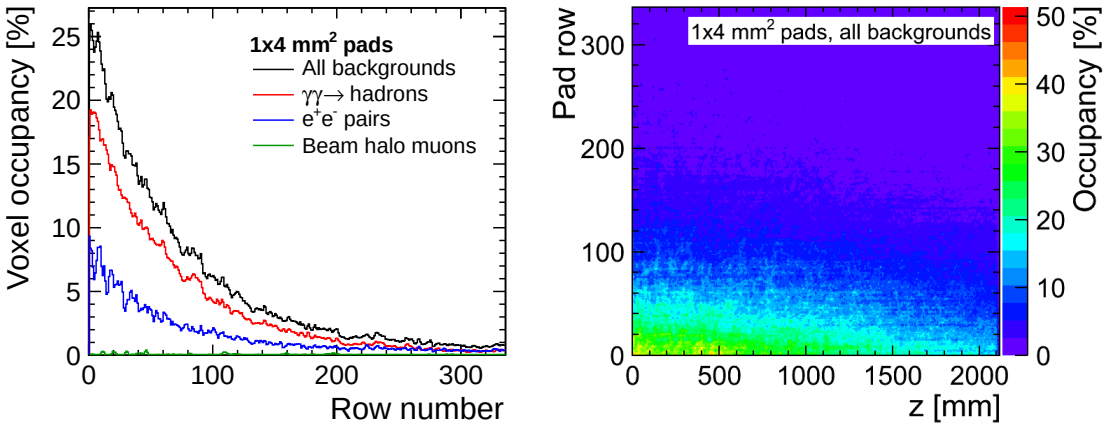


(a) The voxel occupancy calculated per pad row.

(b) The voxel occupancy calculated per pad row and $z$ bin.

Figure 13: The TPC's voxel occupancy for one bunch train of the different background components as a function of the pad row, and as a function of the pad row and $z$ for all background components. The values are calculated for a pad size of $1 \times 4$ mm$^2$.

| Background | Pad rows | Occupancy [%] | ( nOccupied / nVoxels) |
|---|---|---|---|
| all | all | 3.57 | (86,470,896 / 2,419,106,598) |
| | inner 10 | 24.7 | ( 6,917,702 / 27,999,180) |
| $\gamma\gamma \to$ hadrons | all | 2.51 | (60,721,688 / 2,419,106,598) |
| | inner 10 | 18.4 | ( 5,144,793 / 27,999,180) |
| $e^+e^-$ pairs | all | 1.10 | (26,716,696 / 2,419,106,598) |
| | inner 10 | 7.81 | ( 2,186,402 / 27,999,180) |
| beam halo muons | all | 0.040 | ( 963,761 / 2,419,106,598) |
| | inner 10 | 0.035 | ( 9,855 / 27,999,180) |

Table 5: The average voxel occupancies in the TPC for the different types of beam induced background at a pad size of $1 \times 4$ mm$^2$.

## A.2. $1 \times 1$ mm$^2$ Pads

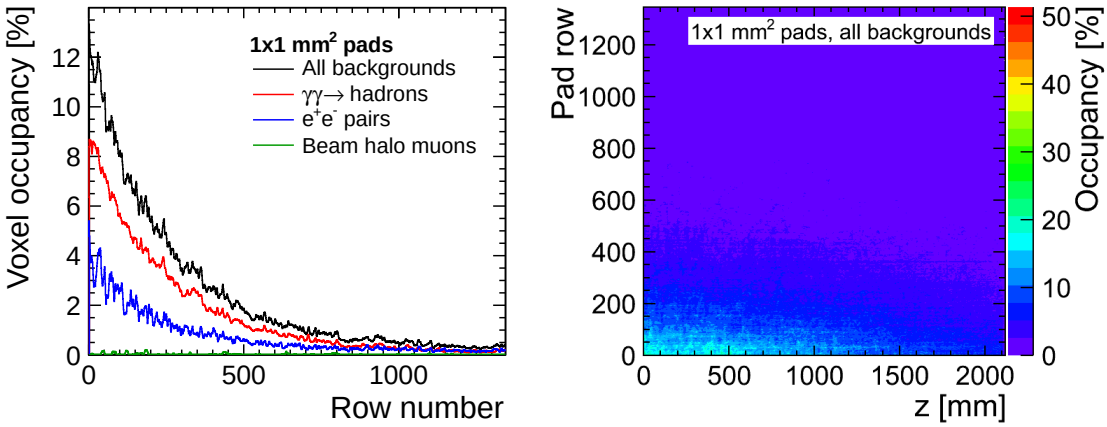


(a) The voxel occupancy calculated per pad row.

(b) The voxel occupancy calculated per pad row and $z$ bin.

Figure 14: The TPC's voxel occupancy for one bunch train of the different background components as a function of the pad row, and as a function of the pad row and $z$ for all background components. The values are calculated for a pad size of $1 \times 1$ mm$^2$.

| Background | Pad rows | Occupancy [%] | ( nOccupied / nVoxels) |
|---|---|---|---|
| all | all | 1.57 | (152,015,593 / 9,676,430,688) |
| | inner 10 | 12.2 | ( 3,302,733 / 26,986,398) |
| $\gamma\gamma \to$ hadrons | all | 1.05 | (102,014,134 / 9,676,430,688) |
| | inner 10 | 8.29 | ( 2,237,351 / 26,986,398) |
| $e^+e^-$ pairs | all | 0.514 | ( 49,709,180 / 9,676,430,688) |
| | inner 10 | 4.29 | ( 1,158,400 / 26,986,398) |
| beam halo muons | all | 0.018 | ( 1,706,308 / 9,676,430,688) |
| | inner 10 | 0.015 | ( 4,025 / 26,986,398) |

Table 6: The average voxel occupancies in the TPC for the different types of beam induced background at a pad size of $1 \times 1$ mm$^2$.

# B. Software List

This sections lists the software which has been used for this study. A detailed description of the packages and a list of all the parameters can be found in a dedicated note [4].

## B.1. Simulation

Mokka with the `CLIC_ILD_CDR` detector model, the `clictpc01swl` TPC subdetector and the `FieldMap4TNoQuad` magnetic field.

## B.2. Digitisation

The digitisation is performed in Marlin, using the MarlinTPC package for TPC studies.

- `OverlayProcessor` or `OverlayIncoherentPairsProcessor`[4)]
- `DriftProcessor`
- `GEMProcessor`
- `ChargeDistributionProcessor`
- `TPCElectronicsProcessor`
- `OverlayRawDataProcessor`
- `MergeRawDataProcessor`

## B.3. Reconstruction

These data have not been reconstructed. The occupancy calculation directly runs on the digitisation output.

[4]The incoherent pairs consist of 300,000 Mokka events per bunch crossing, which result in three input LCIO input files per bunch crossing. It was impracticable to use the `OverlayProcessor` with this. The `OverlayIncoherentPairsProcessor` reads in three files per bunch crossing and puts all events in them into one LCIO event. The overlaying functionality is the same as the `OverlayProcessor`.